Distortion-Dependent Unhooking of Interstrand Cross-Links in Mammalian Cell Extracts†

Michael B. Smeaton,‡ Erica M. Hlavin,‡ Tracey McGregor Mason,‡ Anne M. Noronha,§ Christopher J. Wilds,§ and Paul S. Miller*,‡

Department of Biochemistry and Molecular Biology, Johns Hopkins Bloomberg School of Public Health, Johns Hopkins University, 615 North Wolfe Street, Baltimore, Maryland 21205, and Department of Chemistry and Biochemistry, Concordia University, Montreal, Quebec, Canada

Received May 16, 2008; Revised Manuscript Received July 18, 2008

ABSTRACT: Interstrand cross-links (ICLs) are formed by many chemotherapeutic agents and may also arise endogenously. The mechanisms used to repair these lesions remain unclear in mammalian cells. Repair in *Escherichia coli* and *Saccharomyces cerevisiae* requires an initial unhooking step to release the tethered DNA strands. We used a panel of linear substrates containing different site-specific ICLs to characterize how structure affects ICL processing in mammalian cell extracts. We demonstrate that ICL-induced distortions affect NER-dependent and -independent processing events. The NER-dependent pathway produces dual incisions 5′ to the site of the ICL as described previously [Bessho, T., et al. (1997) *Mol. Cell. Biol. 17* (12), 6822−6830] but does not release the cross-link. Surprisingly, we also found that the interstrand cross-linked duplexes were unhooked in mammalian cell extracts in a manner independent of the NER pathway. Unhooking occurred identically in extracts prepared from human and rodent cells and is dependent on ATP hydrolysis and metal ions. The structure of the unhooked product was characterized and was found to contain the remnant of the cross-link. Both the NER-mediated dual 5′ incisions and unhooking reactions were greatly stimulated by ICL-induced distortions, including increased local flexibility and disruption of base pairs surrounding the site of the ICL. These results suggest that in DNA not undergoing transcription or replication, distortions induced by the presence of an ICL could contribute significantly to initial cross-link recognition and processing.

Interstrand cross-links (ICLs)[1] covalently tether both strands of the DNA duplex, preventing strand separation and therefore transcription and replication (*1*). This modification poses a unique challenge to the cellular DNA repair machinery because a nondamaged template is not readily available during repair synthesis. An understanding of ICL repair pathways has important clinical implications in chemotherapy as well as aging (*1*−*3*).

Much of what is known about the mechanisms of ICL repair has come from studies in *Escherichia coli* and *Saccharomyces cerevisiae*, where repair is initiated by the nucleotide excision repair (NER) pathway (*1, 4, 5*). NER-dependent incisions are made on either side of the cross-link, thereby "unhooking" the two DNA strands. Unhooking is then followed by error-free or error-prone repair of the ICL utilizing either homologous recombination (HR) or translesion synthesis (TLS) pathways. NER can then remove the residual damage on the other strand.

Repair of ICLs in mammals is quite complex and involves many different proteins from different repair pathways. Although the precise mechanisms are still unknown, it is clear that proteins in the NER pathway play an important role in this process (*1*). Mammalian cell lines that are mutated for the XPF-ERCC1 factor, but not other NER proteins, are hypersensitive to cross-linking agents and appear to be defective in the unhooking step as measured by a comet assay (*6*). Other studies have implicated an ICL repair mechanism that uses the entire NER pathway (*7*−*9*).

Mechanistic studies in mammalian whole-cell extracts (WCEs) using a defined psoralen cross-linked lesion have demonstrated that the NER pathway makes dual incisions on the 5′ side of the ICL, leaving the cross-link intact and producing a gap that is filled by a "futile" repair synthesis process (*10, 11*). Others have observed incisions surrounding a psoralen ICL that are produced in a manner dependent upon XPF-ERCC1 and Fanconi anemia (FA) proteins (*12, 13*). However, the mechanisms used to initiate repair of ICLs in mammals remain unclear.

Lesion-induced helix distortions appear to be involved in the recognition of DNA damage by many DNA repair proteins, including those of the NER pathway (*14, 15*). It is still not known, however, if or how ICL-induced helical distortions affect repair processing of this clinically important DNA lesion. We have reported previously on the syntheses and structures of a series of interstrand cross-linked duplexes

† This research was supported by a grant from the National Cancer Institute (CA082785). T.M.M. was supported by a National Research Service Award (CA108326).

* To whom correspondence should be addressed. E-mail: pmiller@jhsph.edu. Phone: (410) 955-3489. Fax: (410) 955-2926.

‡ Johns Hopkins University.

§ Concordia University.

[1] Abbreviations: ICL, interstrand cross-link; NER, nucleotide excision repair; AMT, 4′-aminomethyl-4,5′,8-trimethylpsoralen; TBE, Tris/borate/EDTA; PNK, polynucleotide kinase; TE, Tris/EDTA.

10.1021/bi800925e CCC: $40.75
Published on Web 08/15/2008

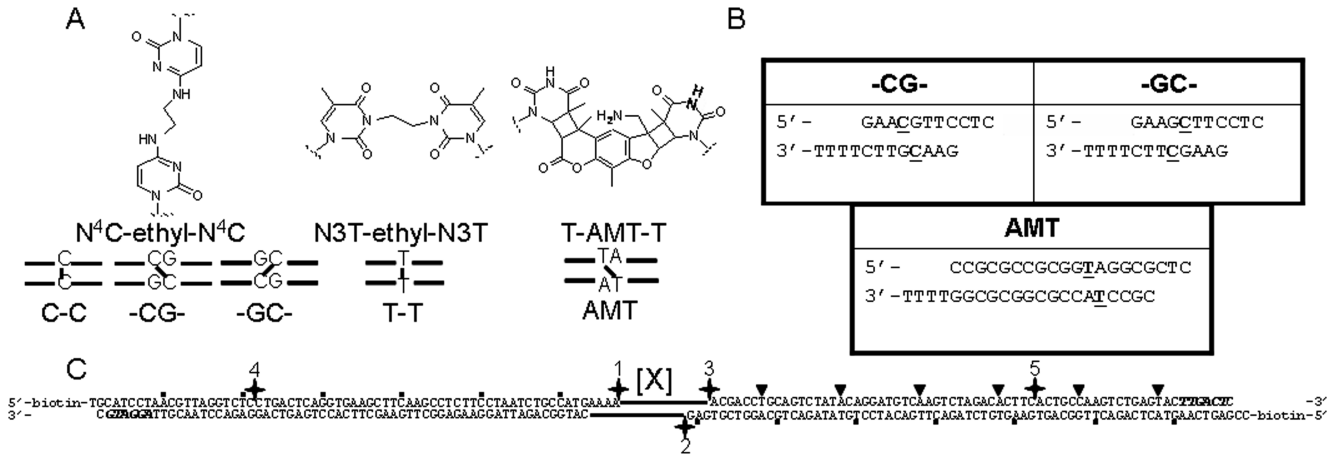

FIGURE 1: Substrates used in this study. (A) Schematic of ICLs in which the top left end of each duplex represents the 5′ end. (B) Sequences of cross-linked duplexes used in the incision assays. The underlined nucleotide contains the ICL. (C) Sequence of the full-length substrate where **[X]** denotes the cross-link duplex from panel B ligated in the middle. Bold italic nucleotides contain 3′-methylphosphonate linkages: (star) ^{32}P label positions 1−5, (■) every 10th base from the 5′ end, and (▼) every 10th base from the 3′ side.

that exhibit various degrees of cross-link-induced distortion of the DNA helix (*16*−*24*). These cross-links, which contain alkyl tethers, serve as models for the types of ICLs that are formed endogenously and by many of the currently used cancer chemotherapeutic agents. Our synthetic procedures allow placement of a chemically identical ICL in different sequence orientations, which generates large variations in DNA duplex distortion. It is this ability that allows us to study how ICL-induced distortions affect cross-link processing.

We hypothesized that helical distortions could affect recognition and repair processing of ICLs. In this report, we use interstrand cross-linked linear DNA duplexes to examine cross-link processing in mammalian whole-cell extracts. These experiments show that the NER-mediated dual incisions are made in a distortion-dependent manner on the 5′ side of the ICLs. Surprisingly, we found that in addition to these NER-mediated 5′ dual incisions, the ICLs are unhooked and this unhooking does not require NER proteins, most notably XPF-ERCC1. We have characterized the structure of the unhooked product and demonstrated that the amount of unhooking is directly influenced by the degree of helix distortion induced by the ICL.

EXPERIMENTAL PROCEDURES

Materials. Protected deoxyribonucleoside 3′-*O*-phosphoramidites, 5′-biotin phosphoramidite, and oligonucleotide synthesis reagents were purchased from Glen Research, Inc. Protected deoxyribonucleoside 3′-*O*-methylphosphoramidites were a product of JBL, Inc. Polynucleotide kinase and T4 DNA ligase were obtained from New England Biolabs, Inc. Reactions employing these enzymes were carried out in buffer supplied by the manufacturer. High-performance liquid chromatography (HPLC) was performed on a Varian instrument using a 0.4 cm × 25 cm Dionex strong anion exchange (SAX) column. MALDI-TOF mass spectra were obtained on an Applied Biosystems Voyager mass spectrometer at the AB Mass Spectrometry/Proteomics Facility, Johns Hopkins School of Medicine, with support from a National Center for Research Resources shared instrumentation grant (1S10-RR14702). Phosphorimage screens were read on a Typhoon 9200 or a Fuji Film FLA-7000 phosphorimager.

Synthesis of Oligonucleotides. The oligonucleotides that comprise the duplexes, whose sequences are listed in Table S1, were synthesized on an Applied Biosystems model 3400 DNA/RNA synthesizer using standard solid-phase phosphoramidite chemistry. Oligonucleotides that contained only phosphodiester linkages were deprotected by treating the support with 400 μL of a 95% ethanol/concentrated ammonium hydroxide solution (1:3, v/v) at 55 °C for 3.5 h. Oligonucleotides that contained 3′-terminal methylphosphonate linkages were deprotected by sequential treatment with a 95% ethanol/concentrated ammonium hydroxide solution (1:3, v/v) for 2.5 h at room temperature followed by treatment with a solution containing 22.5 μL of 95% ethanol, 22.5 μL of acetonitrile, and 50 μL of ethylenediamine for 6 h at room temperature. Oligonucleotides up to 30 nucleotides in length were purified by SAX HPLC using a 30 min linear gradient from 0 to 0.5 M sodium chloride at a flow rate of 1 mL/min. Longer oligonucleotides were purified on 18 cm × 16 cm × 1 mm polyacrylamide gels (20%) run under denaturing conditions (7 M urea in a 1× TBE running buffer). These oligonucleotides were located on the gel by UV shadowing and extracted by incubating the excised gel slice overnight at 37 °C in 1 mL of extraction buffer [20% acetonitrile in 0.1 M ammonium acetate (pH 6.2)]. The buffer was concentrated to 200 μL by evaporation and the oligonucleotide precipitated by the addition of 1 μg of oyster glycogen and 2.5 volumes of 100% ethanol. HPLC and gel-purified oligonucleotides were desalted on C-18 cartridges. The compositions of all the oligonucleotides were confirmed by MALDI-TOF mass spectrometry.

Preparation of Substrates. Synthesis and purification of alkyl cross-linked duplexes containing N^{4}C-ethyl-N^{4}C or N3T-ethyl-N3T ICL were prepared and purified as previously described (*19, 21, 24*). The sequences of the cross-linked duplexes used in the incision assays are shown in Figure 1B. The sequences of the other cross-linked duplexes used in unhooking assays and the duplexes used to prepare full-length substrate are listed in Table S1.

For the 5′ incision assays on the alkyl cross-links, both 5′-hydroxyls of the interstrand cross-linked duplex (positions 1 and 2 in Figure 1C) were labeled with ^{32}P at a specific activity of 3000 Ci/mmol. Duplexes containing the 4′-

aminomethyl-4,5′,8-trimethylpsoralen (AMT) ICL were prepared by annealing their component strands in a buffer containing 10 mM Tris (pH 7.5) and 25 mM NaCl followed by incubation with 10 μM AMT for 10 min on ice followed by irradiation with 365 nm UV light at 4 °C for 20 min. This mixture was used in the ligations, and the AMT interstrand cross-linked substrates were subsequently purified away from non-cross-linked material (see below). For the 5′ incision assays, the top stand of the AMT duplex was first labeled with [^{32}P]phosphate at 6000 Ci/mmol. For the 3′ incision assays, the cross-linked duplexes were phosphorylated with unlabeled ATP and the ^{32}P label was placed at position 3 in Figure 1C by ^{32}P labeling the upper strand of duplex **D** shown in Table S1 at 6000 Ci/mmol. The strands comprising duplexes **A**−**F** (Table S1) were phosphorylated enzymatically by being incubated with T4 polynucleotide kinase in 1× T4 DNA ligase buffer overnight at 37 °C. Preparation of substrates with the label at position 4 or 5 (Figure 1C) was conducted by ^{32}P labeling the top strand of duplex **B** or **F** (Table S1), respectively, and annealing to cold phosphorylated complement before ligation. Complementary oligonucleotides were heated to 65 °C and then annealed by being slowly cooled to room temperature.

The ∼150 bp cross-linked duplexes were prepared by ligating the component duplexes **A**−**F** (Table S1) with the cross-linked duplex **[X]** as previously described (*25*−*27*). Ligations were carried out using 10 pmol of the labeled duplex with 15−20 pmol of each of the cold phosphorylated duplexes. The full-length cross-linked duplexes were purified on an 18 cm × 16 cm × 1 mm polyacrylamide gel (6%) run under denaturing conditions at 60 °C. The full-length product exhibited the slowest mobility and was excised from the gel, incubated with extraction buffer overnight at 37 °C, and recovered by ethanol precipitation. Substrates were resuspended in a solution of 100 mM KCl/1× TE buffer, annealed by being slowly cooled from 90 °C, stored at 4 °C, and used until significant decay of the substrate had occurred.

Cross-linked duplexes used for chemical probing were constructed by ligating cold phosphorylated duplexes A_{cp} and B_{cp} (Table S1) to cold phosphorylated cross-linked duplex **[X]**. The cross-linked duplexes were purified on 16 cm × 18 cm × 1 mm polyacrylamide gels (15%) run under denaturing conditions. Bands containing the full-length duplexes were located on the gel by UV shadowing and extracted from the gel as described above. These substrates were labeled for chemical probing on the 3′ side using exo- Klenow DNA polymerase and the appropriate [α-^{32}P]dNTP.

Chemical Probing. The labeled cross-linked duplex was supplemented with 5 μg of sonicated salmon sperm DNA at a final concentration of 10 mM sodium phosphate buffer (pH 8) with 1 mM EDTA. One microliter of dimethyl sulfate (DMS) or 20 mM potassium permanganate (final concentration) was added to bring the total reaction volume to 100 μL. The DMS and $KMnO_4$ reaction mixtures were incubated for 2 and 20 min, respectively, at room temperature. Both reactions were quenched by the addition of 25 μL of cold stop solution [1.5 M sodium acetate (pH 7), 250 μg/μL tRNA, and 1 M β-mercaptoethanol]. The reaction mixtures were precipitated, washed with cold 70% ethanol, and briefly dried under a vacuum. Each pellet was then treated with 70 μL of 10% aqueous piperidine for 30 min at 90 °C, after which the solution was quickly cooled on ice, and the piperidine was removed by evaporation. The residue was dissolved in denaturing loading buffer (80% formamide, 0.05% xylene cyanol, and 0.05% bromophenol blue); the samples were heated for 2 min at 90 °C, and equal amounts of radioactivity were loaded on a prerun 20% polyacrylamide sequencing gel (20 cm × 45 cm × 0.4 mm) and analyzed by phosphorimaging.

Cell Culture. HeLa cells (Biovest International Inc., National Cell Culture Center) were grown in suspension at densities of 2.5−5 × 10^5 cells/mL in Jolick's minimal essential medium (MEM) supplemented with 5% newborn calf serum, 100 units/mL penicillin, and 100 μg/mL streptomycin. All other cell lines were grown in Eagle's MEM alpha modification, supplemented with 10% fetal bovine serum (FBS), 100 units/mL penicillin, and 100 μg/mL streptomycin. Wild-type Chinese hamster ovary (AA8), UV135 (XPG), UV5 (XPD), and UV61 (CSB) cells were generous gifts from M. Seidman. XPC (GM02246) cells were a gift from the laboratory of L. Grossman. ERCC1 −/− cells (E1KO-7-5) were a gift from R. Nairn. UV41 (XPF) cells were obtained from the American type Culture Collection.

Preparation of Whole-Cell Extracts. Large-scale preparations (∼10^9 cells) of whole-cell extracts were prepared by the method of Manley et al. from HeLa, AA8, UV41, and UV135 cells following previously described procedures (*27*−*29*). A mini-NER whole-cell extract method (*26*) was used to prepare and concentrate extracts from the remainder of the cell lines that were tested. The protein concentrations in the extracts were determined using the Bio-Rad protein assay system and were found to be 15−20 mg/mL (large-scale preparations) or 13−14 mg/mL (mini-NER extracts).

Incision and Unhooking Reactions. Incision and unhooking reactions were carried out using either 5′ or 3′ ^{32}P-labeled duplexes under conditions similar to those described for the in vitro nucleotide excision repair assay (*27, 30*) with minor modifications. The reactions were performed in silanized 1.5 mL Eppendorf tubes in 25 μL of a buffer containing 25 mM HEPES (pH 7.9), 4.4 mM magnesium chloride, 0.1 mM EDTA, 1 mM dithiothreitol, 70 mM potassium chloride, 4 mM ATP, 200 μg/mL bovine serum albumin, 2.5−5% glycerol, 40 ng of pGEM3Z plasmid DNA, and 5−10 μL (75−150 μg) of HeLa whole-cell extract or 5 μL (65−100 μg) of AA8 or mutant extract. Where indicated, mutant extracts were complemented by premixing 2.5 μL of each extract and incubating on ice for 30 min. The biotinylated full-length duplexes (Figure 1C) were mixed with 1 μg of streptavidin per 50 fmol of duplex and incubated overnight at 4 °C prior to incubation with the extracts. The reaction mixtures were set up and held on ice for 15 min and then the reactions initiated by addition of 10 fmol of ^{32}P-labeled cross-linked duplex followed by incubation at 30 °C for 1 h or the indicated amount of time. The reactions were stopped by incubating with 10 μg of proteinase K in the presence of 0.3% SDS for 15 min at 37 °C and then the mixtures extracted with a phenol/chloroform/isoamyl alcohol mixture (25:24:1, v/v) using phase Lock gel tubes (Eppendorf) followed by extraction with a chloroform/isoamyl alcohol mixture (24:1). The DNA was precipitated, washed with 70% ethanol, and dissolved in 10 μL of denaturing loading buffer. For incision reactions, samples were electrophoresed on a prerun (1.5 h) 8% denaturing polyacrylamide sequencing gel

at 1800 V until the bromophenol blue dye was 12 cm from the bottom of the gel. The gel was fixed in a solution containing 5% methanol, 5% acetic acid, and 90% water for 5 min, dried on a gel dryer, and exposed to a phosphorimager screen overnight. For unhooking reactions, the samples were run on a 16 cm × 18 cm × 1 mm denaturing polyacrylamide gel (6%) in a tank with 60 °C 1× TBE buffer filled to cover the gel plates up to the position of the wells. The xylene cyanol tracking dye was run until it was 4 cm from the bottom of the gel. Unhooked products that were shifted with streptavidin were processed as described above, but the samples were bound with 2 μg of streptavidin (Alexa Fluor 555, Invitrogen) for 1 h at room temperature prior to electrophoresis. The excision and unhooking products were quantified and normalized to the total signal in the lane using Image Quant 5.2 or MultiGauge version 3.0. Quantification of the level of excision products was done on samples in which saturation of the signal had not been reached.

Unhooked product was eluted from an excised gel slice as described above. The AMT cross-link was photoreversed by irradiation with 254 nm light for 30 min. The N^4C-ethyl$-N^4C$ cross-link was reversed by incubating the purified unhooked -GC- sample overnight at 60 °C with 10 μL of freshly prepared deamination buffer (2.1 g of $NaHSO_3$, 175 μL of 10 M NaOH, and 25 μL of 2 M hydroquinone dissolved in 5 mL of water). The sample was then precipitated, dissolved in water, and passed through a G-25 spin column to remove excess salt, evaporated, and dissolved in denaturing loading buffer. The mobilities of the unhooked, cross-link-reversed, and control samples were compared on an 8% denaturing sequencing gel which was run until the xylene cyanol tracking dye was ~15 cm from the bottom of the gel.

RESULTS

Interstrand Cross-Linked Substrates. The structures of the ICLs used in this study are shown in Figure 1A: N^4C-ethyl$-N^4C$ in a C−C mismatch or a -CG- or -GC- sequence orientation; N3T−ethyl−N3T in a T−T mismatch; and 4′-amino-4,5′,8-trimethylpsoralen (AMT) in a -TA- sequence orientation. High-resolution structures exist for all of these ICLs except the -GC- ICL, which on the basis of NMR and AFM experiments appears to induce a high level of local flexibility and distortion at the site of the cross-link (*17*). Chemical probing was carried out to further define the structure of this cross-link. As shown in Figure 2, treatment of a labeled -GC- ICL duplex with potassium permanganate ($KMnO_4$), a reagent that probes non-base-paired thymines in DNA, produced new products (marked with an asterisk) corresponding to cleavage at the two thymines 3′ to the ICL on both the top and bottom strands. In contrast, similar probing of a -CG- cross-linked duplex produced the same products as piperidine treatment alone, which indicates no distortions near the site of the -CG- cross-link, a result consistent with high-resolution structural data (*16, 17*). The observed hyperreactivity of the -GC- cross-linked duplex implies significant structural distortions that result in single-stranded-type regions that propagate out two base pairs on either side of the -GC- ICL.

5′ Processing of -CG-, -GC-, and AMT Cross-Linked Duplexes. The sequences of the duplexes containing -CG-, -GC-, or AMT ICLs are shown in Figure 1B. These duplexes, which were used to study 5′ and 3′ processing events, are generically termed duplex **[X]**. They were ligated to six other shorter duplexes [**A**−**F** (Table S1)] to create an ~150 bp substrate with a single site-specific cross-link lesion in the center of the duplex as shown in Figure 1C. A ^{32}P label was placed at one of the positions (1−5) denoted with a star. We have previously shown that modifying the ends of linear DNA substrates with 5′-biotin−streptavidin conjugates and 3′-methylphosphonate linkages significantly enhances the signal of NER-mediated excision of a 1,3-intrastrand d(GTG)−cisplatin lesion in cellular extracts (*25*). We therefore incorporated these modifications into the linear cross-linked duplexes to increase the intensity of the processing signals and to protect the ends of the duplex from digestion by exonucleases.

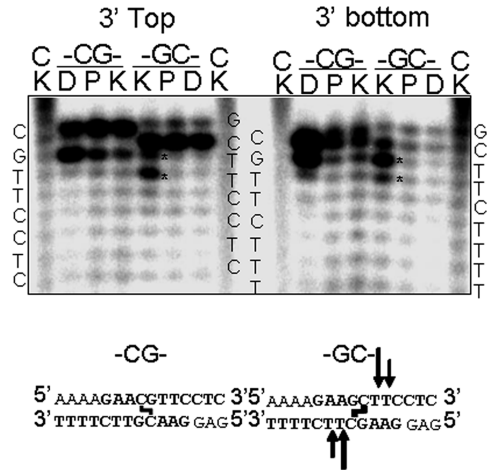

FIGURE 2: Chemical probing of -CG- and -GC- ICLs. Arrows indicate bases susceptible to chemical probes due to structural distortions: K, $KMnO_4$; D, DMS and piperidine; P, piperidine only; C, control non-cross-link.

For the 5′ processing reactions, the short -CG- and -GC-cross-linked duplexes were first end-labeled with [γ-^{32}P]ATP and polynucleotide kinase. After ligation to duplexes **A**−**F**, a full-length substrate with ^{32}P labels at positions 1 and 2 was generated. The top strand of the AMT duplex was ^{32}P-labeled before ICL formation, and therefore, after ligation and purification, the full-length AMT substrate contained a single ^{32}P label at position 1.

As shown in Figure 3 and reported previously (*10*), products 24−32 nucleotides in length were observed, which arose as a result of dual incisions made on the 5′ sides of the -CG-, -GC-, or AMT cross-links by wild-type AA8 or HeLa extracts. There was no change in electrophoretic mobility when the AMT excision products were irradiated with 254 nm light (data not shown), a treatment that reverses the AMT ICL. This confirms that the dual incisions were made on the 5′ side and not on either side of the cross-link. The dual incision products disappeared when the ICL duplexes were incubated with extracts derived from NER-deficient XPF or XPG cells and were restored when the XPF and XPG extracts were mixed (F+G), demonstrating these oligonucleotides are excised by the NER pathway. The level of excision is influenced by the degree of ICL-induced distortion. Thus, the percentage of dual incision product is greater from the highly distorted -GC- duplex (2.4% of the

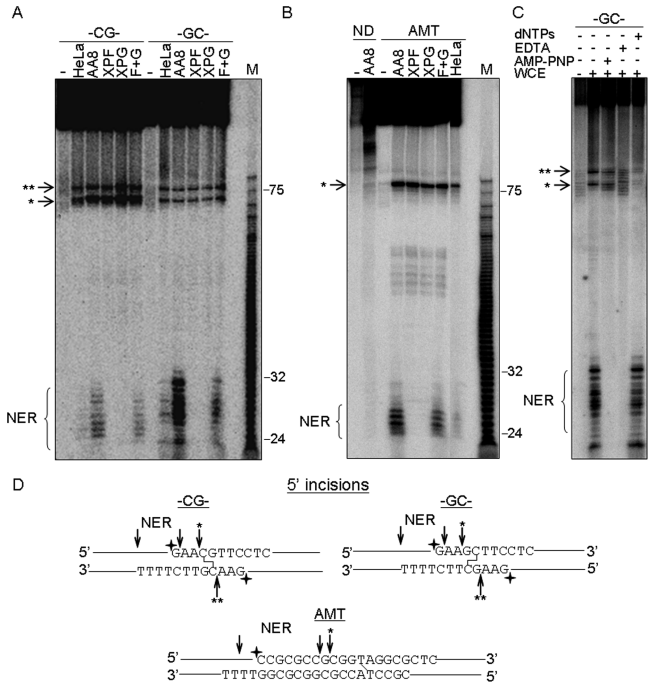

FIGURE 3: Processing of ICL substrates on the 5′ side of the cross-link in mammalian cell extracts. ICL substrates were labeled with ^{32}P on the 5′ side of the (A) -CG- and -GC- ICLs (at positions 1 and 2) or (B) psoralen ICL (position 1) and incubated with wild-type human or CHO (HeLa or AA8, respectively), NER-deficient UV41 (XPF), UV135 (XPG), or a mixture of XPF and XPG (F+G) extracts and then processed and analyzed by denaturing PAGE as described in Experimental Procedures. One and two asterisks denote a single 5′ incision. NER denotes dual 5′ incisions made by the nucleotide excision repair pathway. M denotes molecular weight markers. ND denotes nondamaged substrate with the same sequence as the psoralen ICL duplex. (C) -GC- ICL incubated with AA8 WCE with the indicated modifications to the standard reaction conditions. (D) Schematic illustrating the single 5′ incision locations on -CG-, -GC-, and AMT ICLs (mapped in Figure S2A). The dual NER incision locations were not determined here but were previously for psoralen (*10*). Stars denote the ^{32}P label; arrows indicate the locations of incisions.

total) than from either the -CG- or AMT cross-linked duplexes (~0.7% of the total), which contain only minor distortions.

Additional extract-dependent products, which are marked with a single or double asterisk in panels A and B of Figure 3, were observed close to the 5′ side of the ICL. Because both 5′ arms contain a ^{32}P label and these arms are different lengths (see Figure 1C), two products were observed in Figure 3A that result from processing of either the top (one asterisk) or bottom (two asterisks) strand of the duplex. Only a single product was observed for the AMT duplex (one asterisk), which contains only a single label at position 1 in the top strand (Figure 3B). This observation confirms that the two bands observed in Figure 3A resulted from processing on either the top or bottom strand of the duplex. Unlike the dual incision product, the 5′ incision product was still observed when the duplexes were incubated with XPF or XPG mutant extracts, demonstrating this processing event is NER-independent. The 5′ incision product was not observed when a nondamaged (ND) duplex with the same sequence was incubated with HeLa or AA8 extract, as shown in Figure 3B and in Figure S1A.

The amount of 5′ incision product decreased when the nonhydrolyzable analogue AMP-PNP was substituted for ATP or when EDTA was added to the extract (Figure 3C). As expected, the dual NER incision products completely disappeared under these conditions. Dual incision products were observed when the reaction mixture was supplemented with dNTPs, although the 5′ incision product disappeared (see Discussion).

A summary of the processing events observed on the 5′ side of the ICLs, including the exact cleavage locations of the 5′ incision products (mapped in Figure S2A), is shown in Figure 3D. While we did not map the exact location of the NER incisions in this study, the incision closest to the ICL was shown previously to occur at the third to fifth nucleotide 5′ to the ICL (*10*). NER-mediated dual incisions would preclude observation of the single 5′ product, indicating that these two different types of processing events occur independently on separate molecules. It should be noted that the single 5′ incision occurs on either the top or bottom strand, but not on both strands (see below). These incision events are the main extract-mediated products observed even when the ^{32}P label is placed far from the location of the ICL at position 4 (see Figure S1A). There is a minor product band that migrates as a 58mer and a series of products that migrate like a 45mer. These latter products are the result of NER processing downstream near the site of the cross-link, as the label is at position 4 near the terminal 5′ end.

3′ Processing of -CG-, -GC-, and AMT Cross-Linked Duplexes. Full-length cross-linked duplexes were prepared with a single ^{32}P label on the 3′ side of the cross-link, at position 3 as shown in Figure 1C. Consistent with previous results (*10*), no short oligonucleotides corresponding to NER dual 3′ incisions were observed when these substrates were incubated with mammalian cell extracts (see panels A and B of Figure 4). However, a set of products resulting from processing near the cross-link on the 3′ side were observed for all of the ICLs tested but were not observed on undamaged substrates (Figure 4A,B and Figure S1B). Formation of these 3′ products was not dependent on the NER pathway because the same oligonucleotides were also observed in NER-deficient extracts.

The amounts of 3′ processing products were greatly diminished in the presence of AMP-PNP or EDTA (see Figure 4C), indicating that ATP hydrolysis and metal ions are required for their production. Similar to the single 5′ processing product, the 3′ products were no longer observed when dNTPs were included in the reaction mixture (see Discussion). The exact locations of the 3′ incisions were mapped (Figure S2B) and are shown schematically in Figure 4D. No other 3′ incisions were observed when the label was placed near the 3′ end of the substrate at position *5* (see Figure S1B).

ICL Unhooking in Mammalian Cell Extracts. We reasoned that if mammalian cell extracts were able to make incisions on both the 5′ and 3′ sides of the cross-link, these incisions would unhook the cross-link if both occurred on the same ICL duplex. However, the ability to observe an unhooked product on a denaturing polyacrylamide sequencing gel is hampered by the anomalous mobility of the ICL duplex, which migrates as a smear (see Figure S1A,B). A single-strand 150mer migrates at a position near the center of this smear (data not shown). Therefore, to determine if unhooking of the cross-links occurred, reactions were carried out on an 18 cm × 16 cm × 1 mm denaturing polyacrylamide gel (6%)

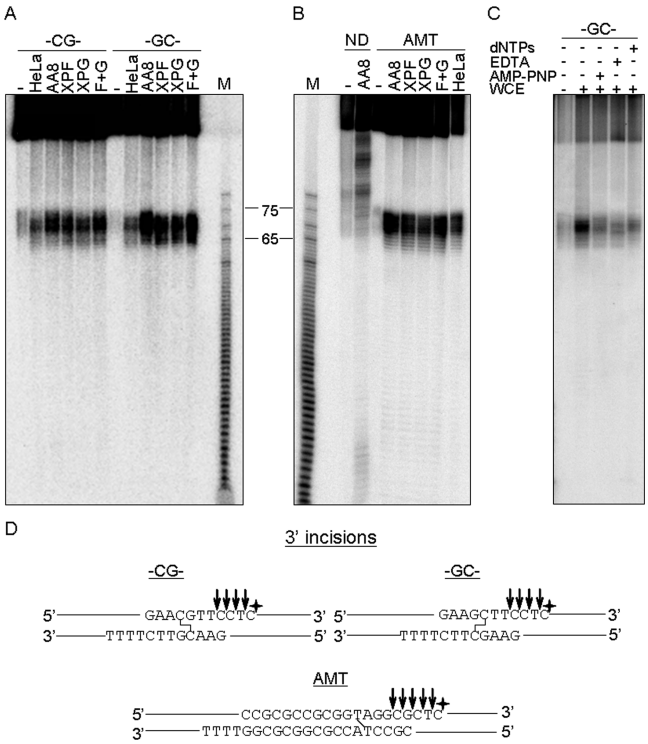

FIGURE 4: Processing of ICL substrates on the 3′ side of the cross-link in mammalian cell extracts. ICL substrates were labeled with ^{32}P on the 3′ side at position 3 of the (A) -CG- and -GC- or (B) psoralen ICL, incubated with wild-type or NER-deficient UV41 (XPF), UV135 (XPG), or a mixture of XPF and XPG (F+G) extracts, and then processed and analyzed by denaturing PAGE as described in Experimental Procedures. (C) The -GC- ICL was incubated with AA8 WCE under the indicated modifications to the standard reaction conditions. (D) Schematic illustrating the exact location of 3′ incisions on -CG-, -GC-, and AMT ICLs (mapped in Figure S1B). Stars denote the ^{32}P label; arrows indicate the locations of incisions.

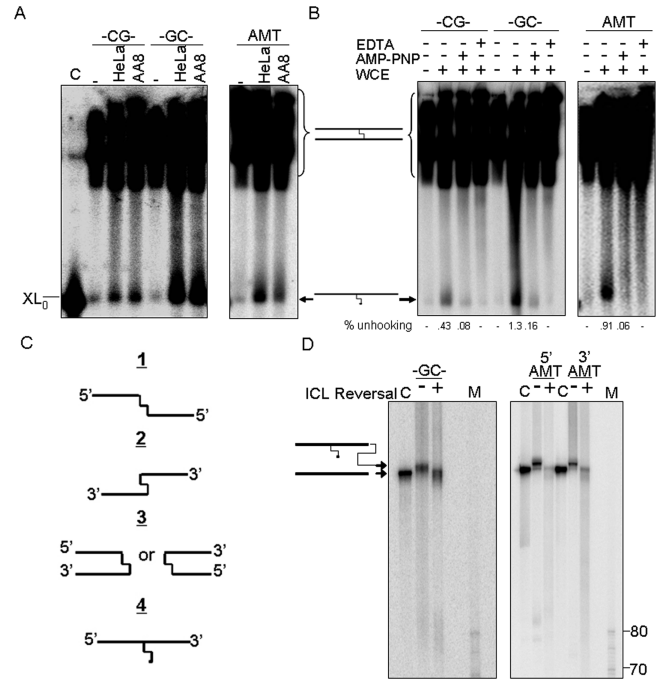

FIGURE 5: Unhooking of ICL substrates in mammalian cell extracts. (A) ^{32}P-labeled ICL substrates were incubated with the indicated WCE and then processed and analyzed on a 6% denaturing gel run at 60 °C. (B) Requirements for the unhooking reaction. The -GC- ICL was incubated with AA8 WCE with the indicated modifications to the standard reaction conditions. The percent unhooked product was determined and is indicated beneath the gel. Quantifications of the unhooking reactions in panel A are shown in Figure 7. (C) Schematic of possible structures of products observed in panels A and B. (D) Characterization of the unhooked product. The unhooked product was gel purified and run on an 8% sequencing gel next to a nondamaged single-stranded control. Half of the purified unhooked product was subjected to reversal of the ICL: GC by sodium bisulfite treatment and psoralen ICL by short wavelength UV. Loss of some sample due to the handling of the reversal treatment resulted in less DNA loaded in the treated lanes. C denotes the nondamaged control.

in a 60 °C heated buffer tank. As shown in Figure 5A, under these conditions, the strands of a non-cross-linked duplex (XL_o) were well separated from a cross-linked duplex of the same length.

When cross-linked duplexes were incubated with HeLa or AA8 whole-cell extract, we observed a product with a mobility similar to that of a single-strand 150mer control (XL_0) as we would expect for unhooking (Figure 5A). No product was observed if the extract was heated to 90 °C, 5 min prior to incubation with the duplexes (data not shown). The unhooking reaction required ATP hydrolysis and metal ions as shown in Figure 5B. The level of unhooked product after each treatment is indicated underneath the gel. In this particular experiment, the percent of unhooked -GC- ICL seen under normal conditions was lower than what we typically observe (such as in Figure 5A). Nevertheless, it is clear that a significant reduction in the level of unhooked product occurs upon incubation with AMP-PNP. Equal amounts of product were observed when the label was placed on either the 5′ or 3′ side of the ICL (Figure S3). Furthermore, as shown for the -GC- cross-linked duplex, addition of dNTPs did not affect the unhooking reaction (Figure S4).

On the basis of its mobility, the reaction product could have one of the structures shown in Figure 5C. To characterize the structure of the unhooked product, we prepared duplexes that contained a -CG- or -GC- oriented cross-link, a single 3′ terminal biotin on the upper strand, and a single ^{32}P label on the upper strand at position 4 near the 5′ end. Only an unhooked, intact top strand (**5C-4**) would contain both the ^{32}P label and biotin. The cross-linked duplexes were incubated with whole-cell extract as described before, but the isolated DNA was mixed with streptavidin just before electrophoresis. As shown in Figure S3, the mobility of the product band was reduced in the presence of streptavidin, similar to that of a control. A reciprocal experiment was carried out on a -GC- cross-linked duplex, the top strand of which contained a ^{32}P label at position *5* (near the 3′ end) and a terminal 5′ biotin. As shown in Figure S3, the product band was shifted when streptavidin was added prior to electrophoresis. These results demonstrate the unhooked product has structure **5C-4**.

The unhooked product was isolated from a short 6% polyacrylamide gel, and its mobility on an 8% sequencing gel was compared to that of a non-cross-linked, single-stranded oligonucleotide whose sequence was identical to that of the top strand of the duplex. As shown in Figure 5D, the mobilities of unhooked products derived from both the -GC- and AMT cross-linked duplexes are lower than those of the corresponding nondamaged control. Treatment of the -GC- cross-linked duplex with sodium bisulfite deaminates cytosines and releases the N^4C-ethyl$-N^4C$

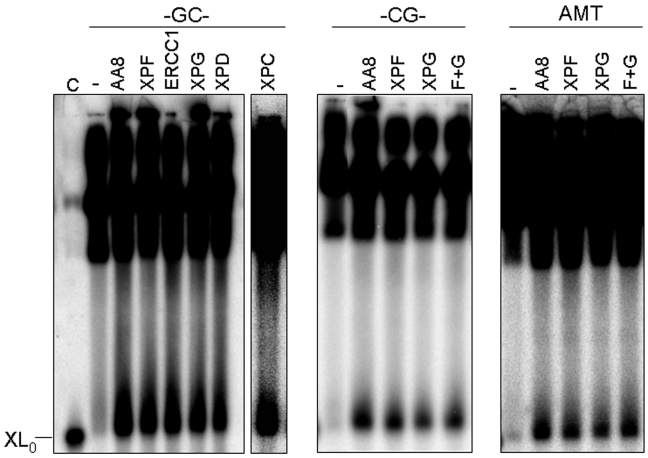

FIGURE 6: Unhooking is independent of NER. Cross-linked substrates were incubated with the indicated NER-deficient extract and processed as described in Experimental Procedures. XL_o denotes the migration position of the non-cross-linked control duplex.

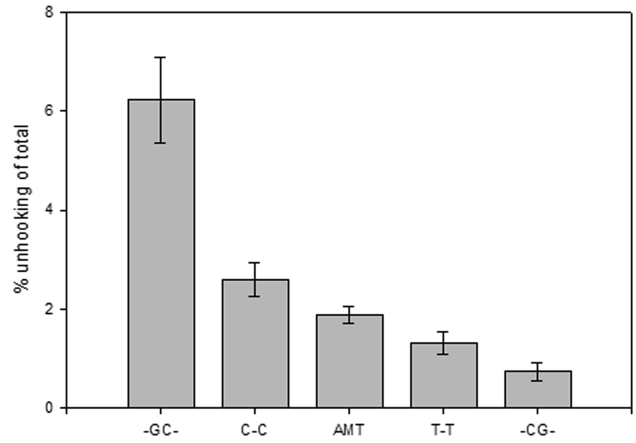

FIGURE 7: Unhooking is influenced by ICL-induced DNA distortions. (A) Three to five reactions with the indicated ICL were carried out in AA8 WCE for 60 min and then the mixtures processed as described in Experimental Procedures. The unhooked product was quantified relative to the total counts loaded. Error bars represent the standard error of the mean.

cross-link (unpublished results). Similarly, UV irradiation (254 nm) of a psoralen cross-linked duplex reverses the cross-link (*10*). When the -GC- and AMT unhooked products were treated with bisulfite and UV light, respectively, their mobilities reverted to that of an unmodified 150mer control, demonstrating that the unhooked product contained the remnant of the cross-link. Cross-link reversal did not create shorter (70−80mer) oligonucleotides, further demonstrating that the unhooked products do not have structure **5C-1**, **5C-2**, or **5C-3**.

The kinetics of the incision and unhooking reactions were examined for the -GC- cross-linked duplex in the hamster AA8 whole-cell extract. As shown in Figure S4, the amounts of the 5′ and 3′ incision products and the unhooked product increased over the course of 4 h and then leveled off. As observed by others, after significant time, the NER-mediated 5′ dual excision products were degraded by exonucleases present in the extract, but the unhooked products were protected due to the end modifications. Approximately 12% of the -GC- duplex was unhooked after 4 h. The unhooking kinetics were not altered in the presence of dNTPs (quantified data not shown).

Unhooking Does Not Require NER Proteins. A mini-NER whole-cell extract method (*26*) was used to prepare extracts from cell lines deficient in the following NER proteins: XPF, ERCC1, XPG, XPD, and XPC. As expected, none of the NER-defective extracts were able to excise a control 1,3-intrastrand d(GTG)−cisplatin lesion (data not shown). However, as shown in Figure 6, all of the mutants were able to unhook the -CG-, -GC-, and AMT ICLs at levels similar to that of wild-type hamster AA8 extract. These results show that the proteins in the NER pathway are not required for the unhooking reaction. Furthermore, the ability of the XPD and XPC extracts to carry out unhooking demonstrates that NER-mediated open complex formation 5′ to the ICL is not required for unhooking. Of particular note was the observation that the XPF mutant cell line UV41 carried out cross-link unhooking (Figure 6). To confirm this result, we tested another cell line (E1KO-7-5) in which the ERCC1 gene is knocked out (*31*). Unhooking was observed in this extract as well. These results indicate that cross-link unhooking does not require XPF-ERCC1. In addition, an extract deficient in CSB, a protein required for transcription-coupled repair, was able to unhook the cross-links (data not shown).

Cross-Link-Induced Helix Distortion Influences Unhooking. When placed in a -CG- orientation, the N^4C−ethyl−N^4C cross-link, which resides in the major groove, is accommodated well by the B-form helix, creates no disruption of base pair H-bonding, and produces a structure that is almost identical to that of the non-cross-linked duplex (*16, 17*). In contrast, when the N^4C−ethyl−N^4C cross-link is placed in the -GC- orientation, the DNA helix is severely distorted because the distance between the two exocyclic amino groups of the cytosines is too great to be spanned by the ethyl group in B-form DNA. These distortions include loss of base pairing by the two nucleotides on either side of the ICL, as determined by chemical probing (Figure 2), and a high degree of flexibility and dynamic motion at the site of the cross-link, as determined by AFM and NMR studies (*16, 17*). The N^4C−ethyl−N^4C cross-link in a mismatched C−C orientation induces a level of distortion intermediate between those of the -CG- and -GC- cross-links: a 27° nonstatic bend in the helix axis and an A-form-like bubble surrounding the site of the cross-link (*22*). Thermodynamically, the -CG- cross-link stabilized the melting temperature of a short duplex by 49 °C relative to that of a non-cross-linked control, whereas the C−C mismatch led to a 25 °C increase relative to the control (*21*). However, the highly distorted -GC- cross-link resulted in a melting temperature 10 °C below that of the control. The mismatched N3T−ethyl−N3T cross-link does not bend or unwind the helix and does not disrupt neighboring base pairs (*20*). Structural studies on AMT and 4,5′,8-trimethylpsoralen cross-linked duplexes demonstrate that this cross-link unwinds the helix by 25° and bends the helix axis approximately 10° while retaining an overall B-form DNA geometry (*32*−*34*). Taken together, the structural data show the relative levels of cross-link-induced distortions decrease in the following order: -GC- > C−C > AMT > T−T ≅ -CG-.

As shown in Figure 5A, for a given cross-link, an equal extent of unhooking was observed in both the HeLa and AA8 extracts. However, comparison of different cross-links reveals that the level of cross-link-induced helix distortion affects

the level of unhooking. Unhooking reactions were carried out in triplicate for 1 h in hamster AA8 whole-cell extracts on duplexes containing each of the ICLs shown in Figure 1A, after which the unhooked products were quantified. The results of these experiments are summarized in Figure 7. After 1 h, 6% of the highly distorted -GC- ICL was unhooked, whereas only 0.7% of the least distorting -CG- ICL was unhooked. Consistent with its level of distortion, unhooking of the C−C cross-link (2.6%) was intermediate between those of the -CG- and -GC- cross-links. Likewise, the AMT cross-link was unhooked at a level intermediate between those of the C−C and -CG- cross-links (1.9%). The T−T ICL was unhooked to an extent similar to that of the nondistorted -CG- ICL. Identical trends were observed when duplexes containing these ICLs were incubated with HeLa whole-cell extracts (data not shown).

To test the unhooking specificity, we carried out reactions on the nondistorted ^{32}P-labeled -CG- duplex in the presence of increasing amounts of unlabeled non-cross-linked duplex (XL_o) or the highly distorted -GC- duplex. As shown in Figure S5, the -GC- duplex competes more effectively than the non-cross-linked duplex. Together, these results indicate that the unhooking reaction is stimulated by ICL-induced helical distortions.

DISCUSSION

There is significant evidence that DNA repair proteins use perturbations of the DNA helix as a means of recognizing damaged DNA (*14*). For instance, the NER pathway, which has the ability to recognize a wide array of bulky adducts in DNA, must rely on a general mechanism of sensing distortions in the DNA helix induced by the presence of damage (*14, 15*). Because most studies that have examined repair of ICLs have used the psoralen ICL, there have been no studies to date that examined the extent to which ICL-induced helical distortions affect the ability of these lesions to be processed by mammalian repair pathways.

We have previously synthesized and characterized a diverse array of site-specific alkyl interstrand cross-links that are analogous to those formed by many chemotherapeutic agents (*16*−*23*). Placing site-specific lesions within linear DNA substrates provides a way of examining repair processing in cell extracts (*27*). We have shown that by modifying the ends of the linear substrates, we can protect the ends from exonuclease degradation and prevent proteins in the extract from binding to the ends of these substrates and consequently interfering with repair (*25*). As a result, these modifications lead to significantly enhanced repair processing signals in cellular extracts. The use of these end modifications along with electrophoretic conditions designed to efficiently separate cross-linked and single-stranded species has allowed us to detect and characterize unhooking of ICLs in mammalian cell extracts (Figure 5). Furthermore, the panel of ICLs has revealed that the level of distortion away from B-form DNA induced by a given ICL, not the chemical nature of the ICL or the physical block to duplex separation, influences both NER-mediated dual 5′ incisions (Figure 3) and unhooking (Figure 8) in mammalian cell extracts.

We have observed two different types of processing of the ICL duplexes as shown schematically in Figure 7. The first results from previously described (*10*) NER-mediated dual incisions made on the 5′ side of the cross-link. While this type of processing does not result in removal of the cross-link, it has been suggested that it may serve to signal further processing of the cross-link by other pathways in the cell (*10*). The efficiency of this 5′ dual incision reaction correlates directly with the degree of helix distortion imparted by the ICL. This is consistent with the known ability of XPC-hHR23B, the mammalian NER recognition factor, to more efficiently bind to and initiate repair of helix-distorting lesions versus nondistorting lesions (reviewed in ref *15*). The crystal structure of the yeast ortholog of XPC bound to DNA damage demonstrates that bases opposite the lesion are flipped out of the DNA duplex (*35*). While it is not possible for the cross-linked bases in an ICL to become completely extrahelical, the ability of bases surrounding the ICL to flip out of the helix may influence the ability of NER and other repair pathways to process ICLs. Consistent with this, the base pairs surrounding the distorted -GC- cross-link, which is recognized more efficiently by the NER machinery than the -CG- ICL, are disrupted, whereas those surrounding the -CG- cross-link are intact (Figure 2 and refs *16* and *17*).

When the NER apparatus encounters a lesion on a single strand, a bubble is created that surrounds the damage and allows incisions to be made on either side of the lesion. The presence of an ICL, which prevents strand separation, would prevent formation of this bubble. This may explain why the NER-mediated dual incisions occur completely 5′ to the site of the ICL. It is still not clear why these incisions occur exclusively on the 5′ side and if or how this processing mediates further repair events.

Interestingly, a second, previously unrecognized type of processing was also observed, which results in unhooking of ICLs and does not require NER proteins. An NER-independent incision appears near the ICL on the 5′ side within one to four nucleotides, depending on the specific ICL. We also observe NER-independent incisions at the fourth through seventh nucleotides 3′ to the ICL. These two incision events must occur on one strand of the duplex to unhook the ICL. The nonincised complementary strand, which contains the remnant of the cross-link, represents the unhooked, full-length single strand from the original duplex (see Figure 8). This unhooking occurs identically in human and rodent cell extracts and is ATP-dependent and metal ion-dependent. Similar to the dual 5′ incisions, this unhooking reaction is also sensitive to ICL-induced helix distortions.

Previous work has shown that both the -CG- and -GC- cross-links are repaired to the same extent in *E. coli* using a reporter plasmid reactivation assay (*17*). Although the level of repair of both cross-links was significantly reduced in NER-deficient cells, an NER-independent repair activity was also observed that was responsive to the level of helix distortion. Using a similar reporter reactivation assay, we have determined that all of the cross-links examined in this work are also repaired in mammalian cells (unpublished results). However, it will be necessary to identify and subsequently ablate the unhooking protein(s) to determine if they are also involved in cross-link repair in these cells.

Studies by others have detected XPF-ERCC1-mediated incisions on the 5′ and 3′ sides of a psoralen ICL in a location similar to those reported here (*12, 13*). However, it is not clear if these incisions occurred on the same molecule and resulted in unhooking. Furthermore, the incisions reported

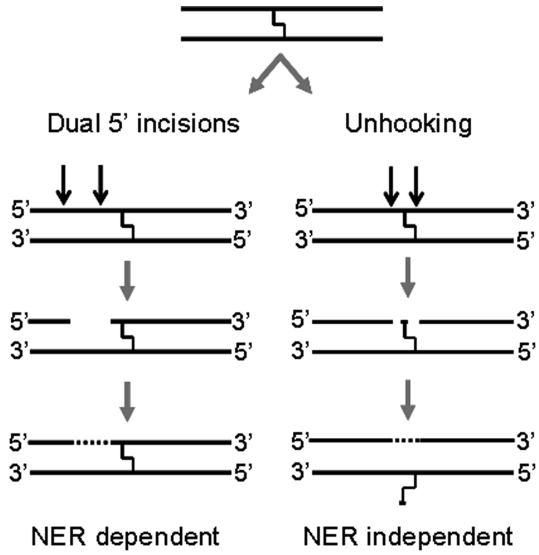

FIGURE 8: Schematic illustrating NER-dependent and -independent processing of ICLs observed in mammalian cell extracts. Both types of processing are sensitive to ICL-induced helical distortions in latent DNA.

here do not require XPF-ERCC1 and therefore appear to represent a separate processing event. Different methods of extract preparation may account for these seemingly different observations.

Unhooking appears to result from processing events on the 5′ and 3′ side of the ICL with a distance of four to seven nucleotides (-CG- and -GC-) or eight to eleven nucleotides (AMT) between incision locations. We have demonstrated that the unhooked product contains the remnant of the cross-link (Figure 5D), although whether this remnant includes an oligonucleotide, such as one that would be produced by two endonucleolytic incisions, or a single nucleotide, that would be produced by one or two endonucleolytic incisions and subsequent exonuclease processing, is currently not known.

Addition of dNTPs to the extracts resulted in the disappearance of the 5′ and 3′ incision products, but not inhibition of cross-link unhooking. As shown schematically in Figure 8, preliminary experiments demonstrate that the gap between the 5′ and 3′ incisions is filled by repair synthesis and ligated (unpublished data). Consequently, addition of dNTPs allows elongation of the 5′ incision product and subsequent ligation to the 3′ incision product, creating a full-length ~150mer strand, a process that results in the complete disappearance of the incision products. The observation that the level of the 5′ and 3′ incision products detected is below that of unhooking (quantified data not shown) is likely due to a low level of dNTPs present in the extract that allows some fill-in and therefore decreased levels of 5′ and 3′ incision products. Consistent with a mode of cross-link recognition independent of replication, addition of dNTPs did not enhance the kinetics or level of unhooking (Figure S4).

There is significant evidence to suggest that the pathway used to repair an ICL may depend upon the manner in which the cross-link is detected. For instance, in cycling cells, cellular sensitivity and Comet assays have implicated XPF-ERCC1 but not other factors in the NER pathway in cross-link repair (*6*). Furthermore, the products of an encounter of a replication fork with an ICL are processed in an XPF-ERCC1-dependent but NER-independent manner (*36*). However, a distinct ICL processing mechanism exists in mammalian cells that requires the transcription-coupled NER pathway (*7*−*9*). It therefore seems that the proteins required to initiate repair of ICLs differ depending on whether the cross-link is encountered during replication or transcription. In both instances, however, XPF-ERCC1 appears to be required for processing. Consistent with this, studies using the purified protein have demonstrated that XPF-ERCC1 can unhook a cross-link in vitro but only if it is placed in a substrate that mimics a stalled fork and not in a fully hybridized DNA (*37*). Alternatively, or in addition to its role in unhooking, the involvement of XPF-ERCC1 in recombination pathways may contribute significantly to the observed sensitivity of cells defective for XPF or ERCC1 (*38*). Surprisingly, the unhooking we describe here is independent of XPF-ERCC1 and appears to represent an alternate ICL processing event independent of replication or transcription. The proteins responsible for unhooking and the relevance of this pathway in vivo remain to be determined. The unhooking activity is, however, analogous to the processing step that initiates repair of ICLs in *E. coli* and *S. cerevisiae* and therefore likely represents a physiologically relevant contribution to repair of ICLs in mammals.

Insight into the distortions recognized by the repair processing pathways shown in Figure 8 comes from examination of the structural features of the most distorted of the cross-links tested, the -GC- and C−C cross-links. The -GC- ICL has the most conformational flexibility and dynamic motion at the site of the cross-link which results in significant bending (*17*). Considering that base stacking interactions are the major force contributing to the rigidity of DNA (*39*), this suggests that base stacking interactions are perturbed in the -GC- ICL. Consistent with this, we have shown here that the base pairs surrounding the -GC- ICL are significantly disrupted (Figure 2). The -GC- ICL is more distorted than the C−C ICL as evidenced by the inability to determine an NMR structure of the -GC- ICL due to excessive conformational changes on the NMR time scale (*17*). The C−C mismatched ICL also experiences conformational flexibility at the site of the ICL along with a nonstatic 27° bend and altered base stacking and base pairing interactions (*22*). These features are observed to a much lesser extent in the other, less distorted cross-links. It therefore appears that flexibility with disruption of base pairing and base stacking interactions surrounding the site of ICLs are important structural determinants for detection of these lesions in DNA not undergoing transcription or replication.

Repair of ICLs can contribute to resistance of tumor cells to chemotherapeutic agents. The cross-links we have used in this study contain an alkyl tether and are similar to those formed by bifunctional alkylating agents such as the nitrogen mustards or nitrosoureas. For example, the N3T−ethyl−N3T ICL mimics the cross-linked formed by bis-chloroethylnitrosourea (BCNU). Although there have been no reports to date of formation of N^4C−alkyl−N^4C interstrand cross-links, mechlorethamine, a nitrogen mustard, has been shown to cross-link cytosines through the N3 position (*40*). In addition, some endogenously derived ICLs, such as those that are formed by reaction with fatty acid metabolites or with certain environmental agents, also form alkyl-type cross-links (*41*). The synthetic ICLs used in our studies have allowed us to demonstrate that the same ICL, N^4C−ethyl−N^4C, is recog-

nized and processed to different extents on the basis of the level of physical distortion it creates when placed in the DNA duplex. An understanding of the types of distortions recognized by mammalian ICL repair pathways may aid in the design of more effective chemotherapeutic agents that can evade repair by tumor cells.

There is a growing body of evidence that formation of endogenously derived ICLs in nondividing, terminally differentiated cells can contribute to aging (*2*). Pathways exist to repair ICL lesions in a G1 context in both yeast (*42, 43*) and mammals (*7*−*9, 44, 45*). In these cells, repair of ICLs in latent DNA or by a transcription-coupled, but not replication-coupled, mechanism would be possible. It is unclear if differences in helical distortion induced by an interstrand cross-link would influence repair by transcription- or replication-coupled mechanisms or if the block to fork progression would promote equal repair for different cross-links. We have shown here, however, that when ICLs are detected and processed in latent DNA, helical distortions significantly affect ICL processing.

ACKNOWLEDGMENT

We thank Dr. Michael Seidman for the generous gifts of cell lines and many helpful discussions. We thank Dr. Lawrence Grossman for the XPC cell line and Dr. Rodney Nairn for the E1KO-7-5 cells. We also thank Ms. Maggie Wear for assistance in preparation of oligonucleotides and members of the Miller laboratory for many helpful discussions and comments.

SUPPORTING INFORMATION AVAILABLE

A description of the oligonucleotides used to prepare the substrates (Table S1), 5′ processing with the ^{32}P label on the far 5′ end and 3′ processing with the ^{32}P label on the far 3′ end (Figure S1), precise location of the incisions made on the 5′ and 3′ sides for the different cross-links (Figure S2), further characterization of the unhooked product structure (Figure S3), the kinetics of the 5′ and 3′ incisions and unhooking with or without addition of dNTPs (Figure S4), and unhooking reaction specific to the ICL as shown via a competition experiment (Figure S5). This material is available free of charge via the Internet at http://pubs.acs.org.

REFERENCES

1. Noll, D. M., Mason, T. M., and Miller, P. S. (2006) Formation and repair of interstrand cross-links in DNA. *Chem. Rev. 106*, 277–301.
2. Grillari, J., Katinger, H., and Voglauer, R. (2007) Contributions of DNA interstrand cross-links to aging of cells and organisms. *Nucleic Acids Res. 35*, 7566–7576.
3. McHugh, P. J., Spanswick, V. J., and Hartley, J. A. (2001) Repair of DNA interstrand crosslinks: Molecular mechanisms and clinical relevance. *Lancet Oncol. 2*, 483–490.
4. Lehoczky, P., McHugh, P. J., and Chovanec, M. (2007) DNA interstrand cross-link repair in *Saccharomyces cerevisiae*. *FEMS Microbiol. Rev. 31*, 109–133.
5. Cole, R. S., and Sinden, R. R. (1975) Repair of cross-linked DNA in *Escherichia coli*. *Basic Life Sci. 5B*, 487–495.
6. De Silva, I. U., McHugh, P. J., Clingen, P. H., and Hartley, J. A. (2000) Defining the roles of nucleotide excision repair and recombination in the repair of DNA interstrand cross-links in mammalian cells. *Mol. Cell. Biol. 20*, 7980–7990.
7. Richards, S., Liu, S. T., Majumdar, A., Liu, J. L., Nairn, R. S., Bernier, M., Maher, V., and Seidman, M. M. (2005) Triplex targeted genomic crosslinks enter separable deletion and base substitution pathways. *Nucleic Acids Res. 33*, 5382–5393.
8. Zheng, H., Wang, X., Warren, A. J., Legerski, R. J., Nairn, R. S., Hamilton, J. W., and Li, L. (2003) Nucleotide excision repair- and polymerase η-mediated error-prone removal of mitomycin C interstrand cross-links. *Mol. Cell. Biol. 23*, 754–761.
9. Wang, X., Peterson, C. A., Zheng, H., Nairn, R. S., Legerski, R. J., and Li, L. (2001) Involvement of nucleotide excision repair in a recombination-independent and error-prone pathway of DNA interstrand cross-link repair. *Mol. Cell. Biol. 21*, 713–720.
10. Bessho, T., Mu, D., and Sancar, A. (1997) Initiation of DNA interstrand cross-link repair in humans: The nucleotide excision repair system makes dual incisions 5′ to the cross-linked base and removes a 22- to 28-nucleotide-long damage-free strand. *Mol. Cell. Biol. 17*, 6822–6830.
11. Mu, D., Bessho, T., Nechev, L. V., Chen, D. J., Harris, T. M., Hearst, J. E., and Sancar, A. (2000) DNA interstrand cross-links induce futile repair synthesis in mammalian cell extracts. *Mol. Cell. Biol. 20*, 2446–2454.
12. Kumaresan, K. R., Sridharan, D. M., McMahon, L. W., and Lambert, M. W. (2007) Deficiency in incisions produced by XPF at the site of a DNA interstrand cross-link in Fanconi anemia cells. *Biochemistry 46*, 14359–14368.
13. Kumaresan, K. R., Hang, B., and Lambert, M. W. (1995) Human endonucleolytic incision of DNA 3′ and 5′ to a site-directed psoralen monoadduct and interstrand cross-link. *J. Biol. Chem. 270*, 30709–30716.
14. Yang, W. (2008) Structure and mechanism for DNA lesion recognition. *Cell Res. 18*, 184–197.
15. Shuck, S. C., Short, E. A., and Turchi, J. J. (2008) Eukaryotic nucleotide excision repair: From understanding mechanisms to influencing biology. *Cell Res. 18*, 64–72.
16. Swenson, M. C., Paranawithana, S. R., Miller, P. S., and Kielkopf, C. L. (2007) Structure of a DNA repair substrate containing an alkyl interstrand cross-link at 1.65 Å resolution. *Biochemistry 46*, 4545–4553.
17. Noll, D. M., Webba da Silva, M., Noronha, A. M., Wilds, C. J., Colvin, O. M., Gamcsik, M. P., and Miller, P. S. (2005) Structure, flexibility, and repair of two different orientations of the same alkyl interstrand DNA cross-link. *Biochemistry 44*, 6764–6775.
18. Wilds, C. J., Noronha, A. M., Robidoux, S., and Miller, P. S. (2005) Synthesis and characterization of DNA duplexes containing an N3T-ethyl-N3T interstrand crosslink in opposite orientations. *Nucleosides, Nucleotides Nucleic Acids 24*, 965–969.
19. Wilds, C. J., Noronha, A. M., Robidoux, S., and Miller, P. S. (2004) Mispair-aligned N3T-alkyl-N3T interstrand cross-linked DNA: Synthesis and characterization of duplexes with interstrand cross-links of variable lengths. *J. Am. Chem. Soc. 126*, 9257–9265.
20. da Silva, M. W., Wilds, C. J., Noronha, A. M., Colvin, O. M., Miller, P. S., and Gamcsik, M. P. (2004) Accommodation of mispair aligned N3T-ethyl-N3T DNA interstrand cross link. *Biochemistry 43*, 12549–12554.
21. Noronha, A. M., Noll, D. M., Wilds, C. J., and Miller, P. S. (2002) N(4)C-ethyl-N(4)C cross-linked DNA: Synthesis and characterization of duplexes with interstrand cross-links of different orientations. *Biochemistry 41*, 760–771.
22. Webba da Silva, M., Noronha, A. M., Noll, D. M., Miller, P. S., Colvin, O. M., and Gamcsik, M. P. (2002) Solution structure of a DNA duplex containing mispair-aligned N4C-ethyl-N4C interstrand cross-linked cytosines. *Biochemistry 41*, 15181–15188.
23. Noll, D. M., Noronha, A. M., and Miller, P. S. (2001) Synthesis and characterization of DNA duplexes containing an N(4)C-ethyl-N(4)C interstrand cross-link. *J. Am. Chem. Soc. 123*, 3405–3411.
24. Noronha, A. M., Noll, D. M., and Miller, P. S. (2001) Syntheses of DNA duplexes containing a C-C interstrand cross-link. *Nucleosides, Nucleotides Nucleic Acids 20*, 1303–1307.
25. Mason, T. M., Smeaton, M. B., Cheung, J. C., Hanakahi, L. A., and Miller, P. S. (2008) End Modification of a Linear DNA Duplex Enhances NER-Mediated Excision of an Internal Pt(II)-Lesion. *Bioconjugate Chem. 19*, 1064–1070.
26. Smeaton, M. B., Miller, P. S., Ketner, G., and Hanakahi, L. A. (2007) Small-scale extracts for the study of nucleotide excision repair and non-homologous end joining. *Nucleic Acids Res. 35*, e152.
27. Reardon, J. T., and Sancar, A. (2006) Purification and characterization of *Escherichia coli* and human nucleotide excision repair enzyme systems. *Methods Enzymol. 408*, 189–213.

28. Wood, R. D. B. M., and Shivji, M. K. K. (1995) Detection and measurement of nucleotide excision repair synthesis by mammalian cell extracts in vitro. *Methods 7*, 163–175.
29. Manley, J. L., Fire, A., Samuels, M., and Sharp, P. A. (1983) In vitro transcription: Whole-cell extract. *Methods Enzymol. 101*, 568–582.
30. Huang, J. C., Zamble, D. B., Reardon, J. T., Lippard, S. J., and Sancar, A. (1994) HMG-domain proteins specifically inhibit the repair of the major DNA adduct of the anticancer drug cisplatin by human excision nuclease. *Proc. Natl. Acad. Sci. U.S.A. 91*, 10394–10398.
31. Adair, G. M., Rolig, R. L., Moore-Faver, D., Zabelshansky, M., Wilson, J. H., and Nairn, R. S. (2000) Role of ERCC1 in removal of long non-homologous tails during targeted homologous recombination. *EMBO J. 19*, 5552–5561.
32. Hwang, G. S., Kim, J. K., and Choi, B. S. (1996) The solution structure of a psoralen cross-linked DNA duplex by NMR and relaxation matrix refinement. *Biochem. Biophys. Res. Commun. 219*, 191–197.
33. Spielmann, H. P., Dwyer, T. J., Sastry, S. S., Hearst, J. E., and Wemmer, D. E. (1995) DNA structural reorganization upon conversion of a psoralen furan-side monoadduct to an interstrand cross-link: Implications for DNA repair. *Proc. Natl. Acad. Sci. U.S.A. 92*, 2345–2349.
34. Spielmann, H. P., Dwyer, T. J., Hearst, J. E., and Wemmer, D. E. (1995) Solution structures of psoralen monoadducted and cross-linked DNA oligomers by NMR spectroscopy and restrained molecular dynamics. *Biochemistry 34*, 12937–12953.
35. Min, J. H., and Pavletich, N. P. (2007) Recognition of DNA damage by the Rad4 nucleotide excision repair protein. *Nature 449*, 570–575.
36. Niedernhofer, L. J., Odijk, H., Budzowska, M., van Drunen, E., Maas, A., Theil, A. F., de Wit, J., Jaspers, N. G., Beverloo, H. B., Hoeijmakers, J. H., and Kanaar, R. (2004) The structure-specific endonuclease Ercc1-Xpf is required to resolve DNA interstrand cross-link-induced double-strand breaks. *Mol. Cell. Biol. 24*, 5776–5787.
37. Kuraoka, I., Kobertz, W. R., Ariza, R. R., Biggerstaff, M., Essigmann, J. M., and Wood, R. D. (2000) Repair of an interstrand DNA cross-link initiated by ERCC1-XPF repair/recombination nuclease. *J. Biol. Chem. 275*, 26632–26636.
38. Bergstralh, D. T., and Sekelsky, J. (2008) Interstrand crosslink repair: Can XPF-ERCC1 be let off the hook? *Trends Genet. 24*, 70–76.
39. Mills, J. B., and Hagerman, P. J. (2004) Origin of the intrinsic rigidity of DNA. *Nucleic Acids Res. 32*, 4055–4059.
40. Romero, R. M., Mitas, M., and Haworth, I. S. (1999) Anomalous cross-linking by mechlorethamine of DNA duplexes containing C-C mismatch pairs. *Biochemistry 38*, 3641–3648.
41. Stone, M. P., Cho, Y. J., Huang, H., Kim, H. Y., Kozekov, I. D., Kozekova, A., Wang, H., Minko, I. G., Lloyd, R. S., Harris, T. M., and Rizzo, C. J. (2008) Interstrand DNA Cross-Links Induced by α,β-Unsaturated Aldehydes Derived from Lipid Peroxidation and Environmental Sources. *Acc. Chem. Res. 41*, 793–804.
42. Sarkar, S., Davies, A. A., Ulrich, H. D., and McHugh, P. J. (2006) DNA interstrand crosslink repair during G1 involves nucleotide excision repair and DNA polymerase ζ. *EMBO J. 25*, 1285–1294.
43. McHugh, P. J., and Sarkar, S. (2006) DNA interstrand cross-link repair in the cell cycle: A critical role for polymerase ζ in G1 phase. *Cell Cycle 5*, 1044–1047.
44. Zhang, N., Kaur, R., Lu, X., Shen, X., Li, L., and Legerski, R. J. (2005) The Pso4 mRNA splicing and DNA repair complex interacts with WRN for processing of DNA interstrand cross-links. *J. Biol. Chem. 280*, 40559–40567.
45. Zhang, N., Lu, X., Zhang, X., Peterson, C. A., and Legerski, R. J. (2002) hMutSβ is required for the recognition and uncoupling of psoralen interstrand cross-links in vitro. *Mol. Cell. Biol. 22*, 2388–2397.

BI800925E